



## FET-based radiation sensors with Er<sub>2</sub>O<sub>3</sub> gate dielectric

S. Kaya<sup>a,b,\*</sup>, A. Jaksic<sup>c</sup>, R. Duane<sup>c</sup>, N. Vasovic<sup>c</sup>, E. Yilmaz<sup>a,b</sup>

<sup>a</sup> Center for Nuclear Radiation Detectors Research and Applications, AIBU, 14280 Bolu, Turkey

<sup>b</sup> Physics Department, Abant İzzet Baysal University, 14280 Bolu, Turkey

<sup>c</sup> Tyndall National Institute, University College Cork, Ireland

### ARTICLE INFO

#### Keywords:

Erbium oxide (Er<sub>2</sub>O<sub>3</sub>)  
High-k materials  
Irradiation effects  
Gamma-ray  
Charge trapping  
pMOS dosimeters

### ABSTRACT

Pre-irradiation device characteristics, gamma radiation response, and possible use in radiation dosimetry have been investigated for MOSFETs with a 100 nm thick Er<sub>2</sub>O<sub>3</sub> gate dielectric. The performance of these novel devices has been compared with that of commercial pMOS dosimeters (RadFETs) with a standard SiO<sub>2</sub> gate oxide of the same thickness. The radiation sensitivity of the Er<sub>2</sub>O<sub>3</sub> is significantly higher than that of SiO<sub>2</sub>, and this is particularly pronounced at lower dose levels. Significantly larger numbers of positive charges are trapped in the Er<sub>2</sub>O<sub>3</sub> dielectric than in SiO<sub>2</sub> during irradiation exposure, resulting in increased threshold voltage shift. After two weeks of room temperature annealing, 11.9% and 24.0% fading have been observed in SiO<sub>2</sub> and Er<sub>2</sub>O<sub>3</sub> samples, respectively. Higher fading for Er<sub>2</sub>O<sub>3</sub> may be related to higher number of shallow traps close to the dielectric/silicon interface. These initial results are promising for the possible use of Er<sub>2</sub>O<sub>3</sub> as a new gate dielectric in pMOS dosimeters. The observed enhancement of device sensitivity can be a milestone for the introduction of the pMOS dosimeters in personal dosimetry applications.

### 1. Introduction

The use of Metal-Oxide-Semiconductor Field-Effect Transistor (MOSFET) as a radiation dosimeter was first reported by Holmes-Siedle [1]; this device is known as RadFET, MOSFET dosimeter, or pMOS dosimeter. The RadFETs have been used in various applications, such as space-radiation dose measurements [2], heavy ion experiments [3], and clinical radiotherapy [4–6]. Instant and non-destructive readout, low power consumption, compatibility with microprocessors, and easy calibration procedures are the main good features that have led to the popularity of these devices [4,7,8].

The operation principle of the RadFETs is based on the radiation induced threshold voltage shift due to charges trapped in the gate oxide, which is a function of absorbed dose [9]. The gate dielectric, which has been a conventional Silicon Dioxide (SiO<sub>2</sub>) layer since device discovery, is the sensitive region for the commercial RadFETs [4,6,7,10]. Researchers have been spending a great effort to enhance the sensitivity of these devices, especially for use as personal dosimeters [7,8,11–14]. The studies have focused on improvement of sensitivity of the standard SiO<sub>2</sub> dielectric by various methods: increase of the dielectric thickness, boron implantation, stacked approaches, etc. However, our previous basic research studies on simple laboratory grown MOS capacitor structures have demonstrated that the use of high-k dielectric materials, such as Aluminum Oxide (Al<sub>2</sub>O<sub>3</sub>) [15], Samarium

Oxide (Sm<sub>2</sub>O<sub>3</sub>) [16], and Erbium Oxide (Er<sub>2</sub>O<sub>3</sub>) [17] can increase radiation sensitivity of the oxide- layer. The SiO<sub>2</sub> is more cost effective and technology compatible layer than potential high- k materials. The minimal detectable dose for single SiO<sub>2</sub> based NürFETs is around the few mGy. This sensitivity is useful for the space and high energy physics applications where high irradiation field exist. However, requirement radiation sensitivity of dosimeters should be improved for the medical applications and must reach to few µGy for devices to be used in personal dosimetry for workers [18]. Hence, different materials should be investigated in order to enhance radiation sensitivity of the FET based detectors. The previous reported MOS studies mentioned above with high- k materials were in form of laboratory grown simple capacitor structures. The responses of fully processed MOS transistors with high-k gate stacks under realistic semiconductor processing conditions have not been studied so far. Hence, among previously investigated high-k materials, Er<sub>2</sub>O<sub>3</sub> has been selected as one of the most promising materials, with low initial interface trap density, thermal stability with Si, and high offset values [17,19–24]. The Er<sub>2</sub>O<sub>3</sub> pMOS transistors were fabricated in the Abant İzzet Baysal University Nuclear Radiation Detectors Research and Applications Center (NÜRDAM), Bolu, Turkey; and we call these devices NürFETs. In the present, study the pre-irradiation characteristics and radiation response of Er<sub>2</sub>O<sub>3</sub> NürFETs has been investigated with the view of a possible use in radiation dosimetry. The performance of Er<sub>2</sub>O<sub>3</sub> NürFETs has been compared with that

\* Corresponding author at: Center for Nuclear Radiation Detectors Research and Applications, AIBU, 14280 Bolu, Turkey.  
E-mail address: [senolkaya52@gmail.com](mailto:senolkaya52@gmail.com) (S. Kaya).

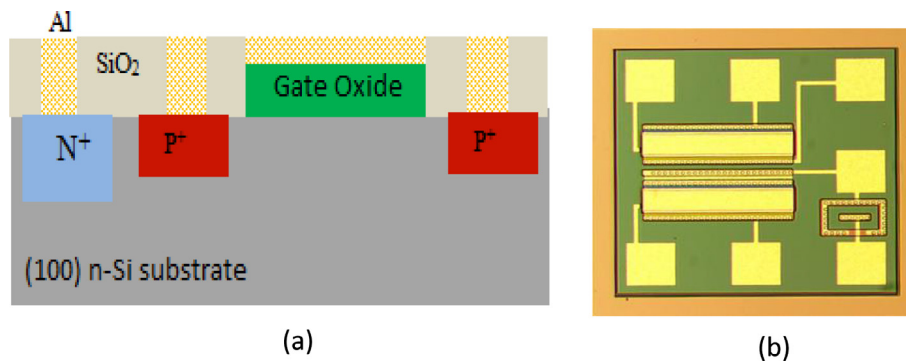


Fig. 1. Fabricated NürFETs (a) schematic cross section, and (b) images under metallurgical microscope.

of standard commercial SiO<sub>2</sub> RadFETs fabricated in Tyndall National Institute, Ireland.

## 2. Experimental details

### 2.1. Device fabrication

The Nuclear Radiation Sensing Field Effect Transistors (NürFETs) with the Er<sub>2</sub>O<sub>3</sub> gate dielectric were fabricated by Abant İzzet Baysal University Nuclear Radiation Detectors Research and Applications Center, Bolu, Turkey. The schematic structure and images under the metallurgical microscope of fabricated devices are depicted in Fig. 1(a) and (b), respectively. Each chip contains two individual NürFETs with a channel width of  $W = 300 \mu\text{m}$  and a channel length of  $L = 50 \mu\text{m}$ . One of NürFET has a common substrate pin, while the other terminals are independent. The other NürFET source and bulk terminals are internally connected, while drain and gate terminals are independent. During the fabrication process, six-inch (100) n-type Si wafers with the resistivity of 1–4 Ohm-cm were used as starting material. Following the Radio Corporation of America (RCA) cleaning process, a field oxide layer of approx.  $1 \mu\text{m}$  was grown by wet oxidation at  $1100^\circ\text{C}$ . The photolithography and wet-chemical etching were carried out to define doped areas. The n<sup>+</sup>-doped regions were formed by phosphorus diffusion (using POCl<sub>3</sub>), and p<sup>+</sup>-regions were formed by boron diffusion (using BBr<sub>3</sub>). Another lithography, wet etching and RCA cleaning process were performed respectively to form channels where Er<sub>2</sub>O<sub>3</sub> gate dielectric layer was deposited. Following the gate channel formation, the Er<sub>2</sub>O<sub>3</sub> gate dielectric layer was deposited by RF sputtering. During the sputtering process a 99.99% pure four-inch Er<sub>2</sub>O<sub>3</sub> target was used and the sputtering power was adjusted to 300 W with 16 sccm ultrapure Ar flow. To study structural and morphological characteristics of the gate dielectric, the Er<sub>2</sub>O<sub>3</sub> layers were also deposited on separate similar Si wafers following the same procedure. After the deposition, the devices and deposited films were annealed at  $350^\circ\text{C}$  in nitrogen for 30 min. The thicknesses of the dielectric layers were measured to be 100 nm using spectroscopic reflectometer. Crystallographic structure and gate dielectric morphology were investigated by X-ray diffractometry (XRD) and Atomic Force microscopy (AFM), respectively. Aluminum was used for metallization procedure and then the post-metallization anneal was performed at  $150^\circ\text{C}$  for 30 min in the presence of Nitrogen to complete Er<sub>2</sub>O<sub>3</sub> NürFET fabrication. In order to compare device specifications and to discuss possible use of Er<sub>2</sub>O<sub>3</sub> NürFETs as radiation dosimeters, commercial p-channel RadFETs with 100 nm SiO<sub>2</sub> gate dielectric, fabricated by Tyndall National Institute – Ireland, were also used in this study.

### 2.2. Electrical characterizations and irradiation test

Transfer characteristics ( $I_d - V_{gs}$ ) and charge pumping curves were measured to determine initial (pre-irradiation) device characteristics.

Using the initial device characteristics including the interface trap density and threshold voltage, usability of Er<sub>2</sub>O<sub>3</sub> NürFETs in micro-electronic applications has been discussed. During the irradiation experiment four Er<sub>2</sub>O<sub>3</sub> and four Tyndall pMOS samples were used. The samples were exposed to several Co-60 gamma irradiation doses up to 1600 Gy with a certificated Ob-Servo Sanguis Co-60 gamma irradiator with approximate dose rate of 417 Gy/h in the Turkish Atomic Energy Authority Gamma Irradiation Facility. The devices were irradiated with zero gate bias (all terminals grounded) during irradiation. Threshold voltage ( $V_{th}$ ) values were determined by using constant-current methods [25], i.e.,  $V_{th}$  values were determined as voltage values at the specified current level ( $10 \mu\text{A}$  for SiO<sub>2</sub> RadFETs, and  $1 \mu\text{A}$  for Er<sub>2</sub>O<sub>3</sub> NürFETs). In addition, transfer characteristics ( $I_d - V_{gs}$ ) were measured before irradiation and after each dose step. The McWhorter and Winokur's [26] midgap sub-threshold charge separation technique was used to calculate radiation-induced trap densities. The threshold voltage recovery (fading) characteristics of the devices during room temperature annealing were also investigated.

## 3. Results and discussion

### 3.1. Pre-Irradiation characterization

The crystallographic and morphological parameters of dielectric layers directly influence electrical properties of devices [27–29]. Therefore, the analysis of these parameters should be considered to enhance reliability of the study. The XRD and AFM measurements are given in Fig. 2(a) and (b) for Er<sub>2</sub>O<sub>3</sub>/Si films to observe the annealing effects. The peaks were indexed by International Centre for Diffraction Data (ICDD) base and the indexed peaks are in agreement with the peaks of the Er<sub>2</sub>O<sub>3</sub> cubic phase with card no: 77-0463 [17]. It was observed the films were highly oriented in (222) and (444) orientations and minor peaks intensities were vaguely seen in enlargement of the XRD scans. Presence of strain and stress on the films may influence the crystalline orientation of the deposited layer [30]. Hence, possible stress and strains on the film may influence crystallographic orientation of the Er<sub>2</sub>O<sub>3</sub> layer. In addition, the grain size of the films was calculated from boarding of intense peak (222) using Scherrer's equation [17,31] to be 22.15 nm. On the other hand, the AFM measurement is depicted in Fig. 2(b). The surface roughness ( $R_q$ ) was calculated to be 2.8 nm. The calculated  $R_q$  is relatively low compared to the Er<sub>2</sub>O<sub>3</sub> thin films deposited by PVD methods [32,33], indicating uniform surface morphology has been obtained.

The initial electrical device parameters for assessment of Er<sub>2</sub>O<sub>3</sub> NürFETs use in microelectronics have been analyzed and the obtained results were compared to Tyndall RadFETs having the same thickness of SiO<sub>2</sub> gate dielectric. To do this, the  $I_d - V_{gs}$  transfer characteristics and charge pumping measurements were performed; results are given in Fig. 3(a) and (b), respectively. As expected, no anomalous kinks were observed in the transfer curves, although the large shift toward more

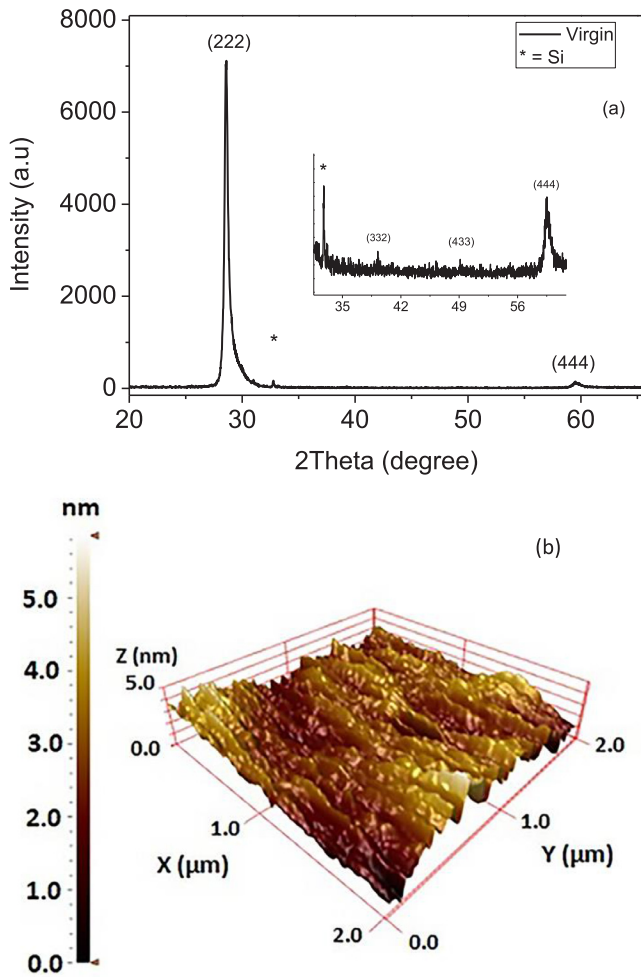


Fig. 2. The a-) XRD of deposited and annealed films, b-) AFM measurements of the annealed  $\text{Er}_2\text{O}_3/\text{Si}$  thin films.

negative values and higher leakage current has been observed at low voltages compared to  $\text{SiO}_2$  RadFETs. The reason for higher transfer current at low voltages is associated with leakage effect [34,35] and the lower slope of the curve is due to trapped charges in the device structure during the fabrication process [36]. The  $V_{\text{th}}$  values for unirradiated devices are given in Table 1. Owing to trapped positive charges during the fabrication and lower dielectric capacitance of  $\text{Er}_2\text{O}_3$  than expected, initial threshold voltages of  $\text{Er}_2\text{O}_3$  NürFETs are higher than that of conventional  $\text{SiO}_2$  RadFETs. Alternative deposition methods, such as Atomic Layer Deposition (ALD), should be used in further studies in order to improve oxide quality and reduce the initial  $V_{\text{th}}$  values [37,38].

In addition, the initial interface trap ( $D_{\text{it}}$ ) were calculated from Eq. (1) [9], using the peak values in charge pumping curves in Fig. 3(b).

$$D_{\text{it}} = \frac{I_{\text{cp,max}}}{f q A} \quad (1)$$

where  $A = L \times W$  is the area under the gate (in our case  $L = 300 \mu\text{m}$ ,  $W = 50 \mu\text{m}$ ),  $f$  is the voltage pulse frequency and  $q$  is the electron charge. The  $D_{\text{it}}$  values for the  $\text{Er}_2\text{O}_3/\text{Si}$  interface are also given in Table 1. This value is close the conventional  $\text{SiO}_2/\text{Si}$  interface trap density and such low  $D_{\text{it}}$  values for  $\text{Er}_2\text{O}_3/\text{Si}$  interface have been also reported in previous studies [17,39]. Considering the pre-irradiation device analysis, despite the higher trapped charge density in the dielectric layer, it was observed that the fabricated  $\text{Er}_2\text{O}_3$  NürFETs were suitable for further investigation.

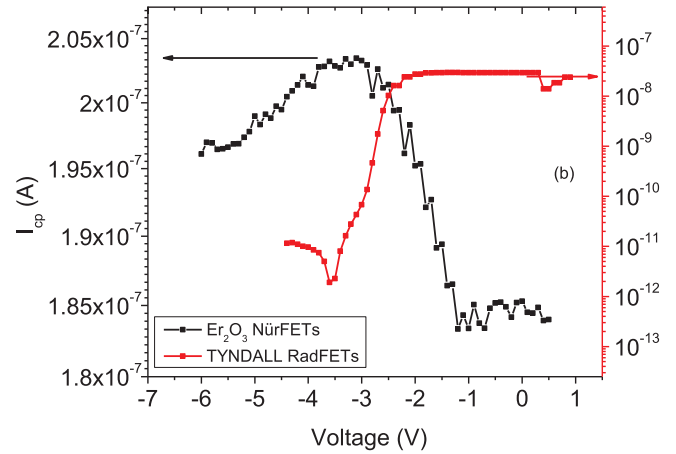
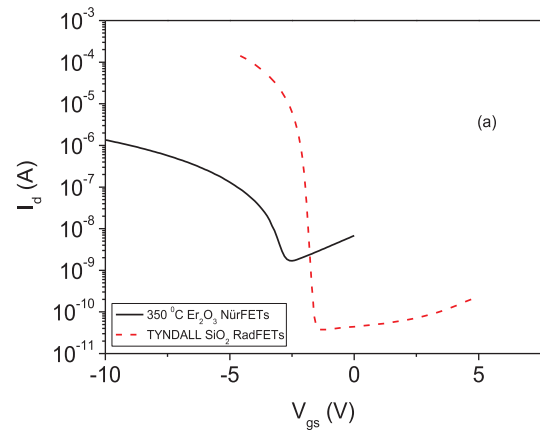


Fig. 3. The (a) transfer  $I_d - V_{\text{gs}}$  characteristics and (b) Charge pumping current measurements of the  $\text{Er}_2\text{O}_3$  NürFETs and Tyndall RadFETs.

Table 1

The  $V_{\text{th}}$  and  $D_{\text{it}}$  parameters of studied devices before irradiation.

	$V_{\text{th}}$ (V)	$D_{\text{it}}$ ( $\times 10^{10} \text{cm}^{-2}$ )
$\text{Er}_2\text{O}_3$ NürFET	-9.00	8.51
$\text{SiO}_2$ RadFET	-2.61	1.05

### 3.2. Irradiation response of devices

The effect of irradiation on electrical  $I_d - V_{\text{gs}}$  characteristics of  $\text{SiO}_2$  RadFETs and  $\text{Er}_2\text{O}_3$  NürFETs are illustrated in Fig. 4(a) and (b), respectively. Threshold voltage shift with the radiation dose is given in Fig. 4(c) for both types of samples. The  $I_d - V_{\text{gs}}$  characteristics of the both devices shift toward more negative voltages. The accumulation of the positive trapped charge densities in the main reason of these observed  $V_{\text{th}}$  shifts [40] which is discussed in details below. Basic mechanism of the irradiation induced effects for  $\text{SiO}_2$  gate dielectric is well-known [41,42]. Briefly, the irradiation generates number of new defects and electron-hole (e-h) pairs. Owing to higher mobility of electron, they are easily swept out from the gate, while holes which escape initial recombination move toward  $\text{SiO}_2/\text{Si}$  interface where deep traps are located. The radiation-induced defects and the trapped holes cause the shifts in threshold voltages as seen in Fig. 4(a). Similar negative voltage shift in the  $\text{Er}_2\text{O}_3$  NürFETs under irradiation exposure indicates that the holes are trapped in the device structure [8,9,17,42]. Generation of oxygen vacancies under radiation exposure have been confirmed by our previous  $\text{Er}_2\text{O}_3$  thin film study [43]. The oxygen vacancies have been known as hole trap centers [44,45]. Hence, the continuous negative threshold voltage shift for  $\text{Er}_2\text{O}_3$  NürFETs can be

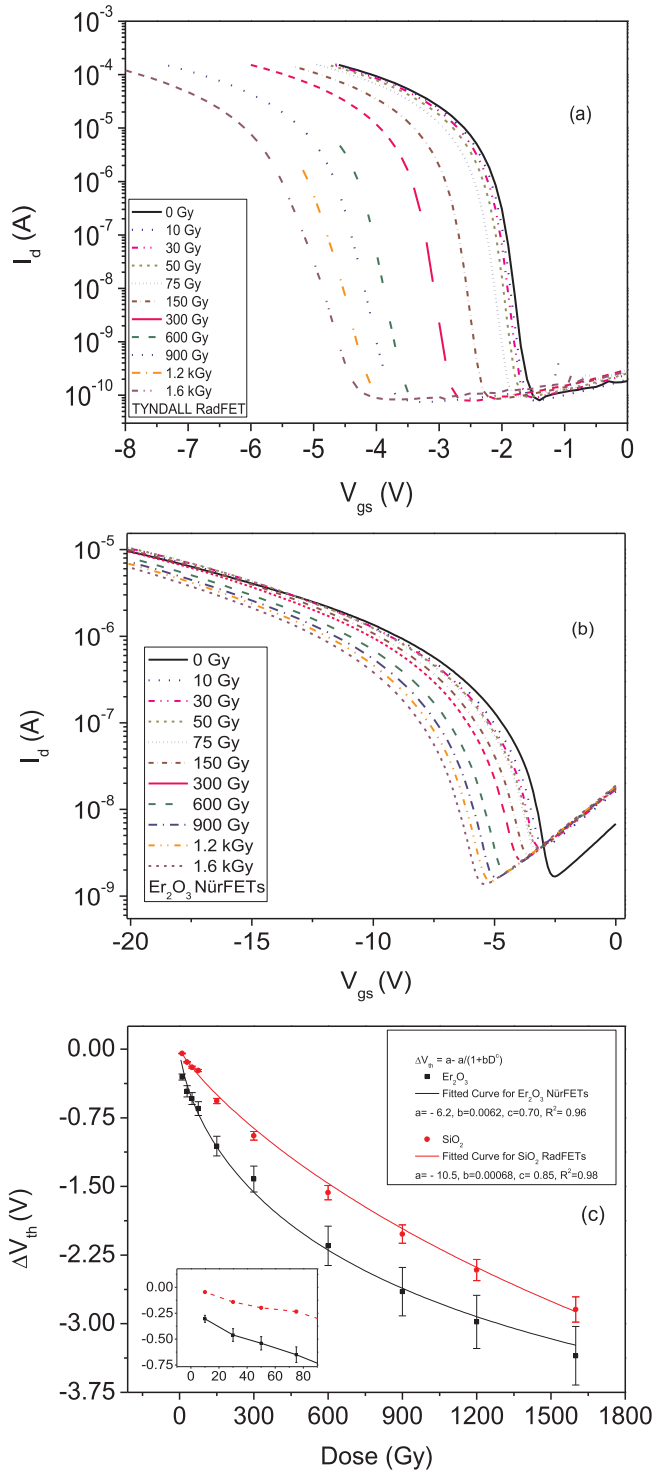


Fig. 4. The  $I_d - V_{gs}$  transfer characteristics of (a) Tyndall RadFETs, (b)  $Er_2O_3$  NurFETs during irradiation, and (c) Threshold voltage shift dose relations for the devices.

attributed to generation of oxygen vacancies under irradiation.

The fitted curves describing shifts in the threshold voltage ( $\Delta V_{th}$ ) – dose relationship are shown in Fig. 4(c). Similar trend was observed for both samples. Relatively large standard deviations shown in error bars for  $Er_2O_3$  NurFETs are probably associated with device-to-device in process variations during the  $Er_2O_3$  deposition by sputtering [46]. The radiation-induced shift in  $V_{th}$  (in Fig. 4(c)) can be expressed by a fitted non-linear Equation [9]:

$$\Delta V_{th} = a - \frac{a}{1 + bD^c} \quad (2)$$

The values of the fitting coefficients,  $a$ ,  $b$ , and  $c$ , are shown in the inset in Fig. 4(c). The linearity of the  $\Delta V_{th}$  – dose relationship of the devices decreases at higher doses. The accumulation of positive radiation-induced oxide trapped charge leads to electric field screening at higher doses, causing the sub-linear behavior of the sensor [4,5]. The radiation sensitivity ( $S = \Delta V_{th}/D$ ) of the  $Er_2O_3$  is higher than that of  $SiO_2$ , and this is particularly pronounced at lower dose levels. For example, sensitivity of  $Er_2O_3$  NurFETs at 30 Gy is 15 mV/Gy vs. only 4.6 mV/Gy for  $SiO_2$  RadFETs. However, the  $SiO_2$  RadFET's response is more linear with those than  $Er_2O_3$  NurFET's comparing the goodness of fitness values ( $R^2$ ) [4]. Thus the difference in sensitivities decreases with dose – 7.2 mV/Gy ( $Er_2O_3$ ) vs. 3.8 mV/Gy ( $SiO_2$ ) at 150 Gy, and 2.1 mV/Gy ( $Er_2O_3$ ) vs. 1.88 mV/Gy ( $SiO_2$ ) at 1600 Gy. The data confirms previous findings of significant voltage shifts in irradiated  $Er_2O_3$  capacitor structures [17]. It should be noted that, to the best of our knowledge, these are the first data that show comparable sensitivities of full transistor structures with high- $k$  dielectrics to those with standard  $SiO_2$ . Further investigation will be needed to optimize  $Er_2O_3$  dielectric and reinforce the findings of this initial study; nevertheless it can be concluded that the  $Er_2O_3$  shows excellent promise to replace  $SiO_2$  for MOSFET dosimetry applications.

The radiation sensitivity of the dielectrics depends on several factors, such as the effective atomic number ( $Z_{eff}$ ) of the gate dielectric, film quality, trapping efficiency, etc. Higher  $Z_{eff}$  number increases the probability of the radiation interaction with the material. Hence, larger initial hole yield and larger number of defects, where holes are trapped, can be generated. Higher sensitivity of the  $Er_2O_3$  dielectrics is possibly associated with higher  $Z_{eff}$  value of  $Er_2O_3$  than  $SiO_2$ . It should be noted that  $Z_{eff}$  is not only the factor to enhance radiation sensitivity of devices. Some dielectrics, like  $HfO_2$ , have also higher  $Z_{eff}$  number than  $SiO_2$  but they exhibit lower radiation sensitivity due to charge trapping distribution/efficiency [47]. Trapped charge distribution in high- $k$  gate dielectrics are somewhat more complex to what has been observed in thermal  $SiO_2$  and each dielectric responses should be considered separately [16,48,49].

The irradiation induced oxide trapped charge ( $\Delta N_{ot}$ ) and interface trapped ( $\Delta N_{it}$ ) charge densities during irradiation are shown in Fig. 5(a) and (b), respectively. The  $\Delta N_{ot}$  and  $\Delta N_{it}$  increase with dose for both  $Er_2O_3$  and  $SiO_2$  devices. The sign of trapped charges is positive for both interface traps and oxide trapped charge. However, for some alternative high- $k$  gate dielectrics and its interface underlying the semiconductor layer, such as  $HfO_2/Si$  [46],  $Sm_2O_3/Si$  [16], exhibits both electron/hole trapping and passivation of trapped charges under radiation exposure [47,50]. These bi-directional trap formation and passivation of trapped charges reduce the radiation sensitivity of devices. In these  $Er_2O_3$  samples, the trapping of holes at the trap centers (basically oxygen vacancies in  $Er_2O_3$  [43]) dominates over electron trapping. The continuous generation of holes traps during irradiation significantly contributes to the radiation sensitivity of the  $Er_2O_3$  dielectric layer.

Comparing the  $\Delta N_{ot}$  and  $\Delta N_{it}$  values in Fig. 5, it can be seen that in both type of samples, and particularly in  $Er_2O_3$ , more trapping occurs in the dielectric than at the dielectric/substrate interface. This confirms that the oxide trapped charges are responsible for the  $V_{th}$  shift. Further, the number of both types of radiation-induced oxide and interface trapped charge is significantly higher in  $Er_2O_3$  samples. This is correlated with higher density and  $Z_{eff}$  number of  $Er_2O_3$ , which enhance the radiation absorption probability. The Monte Carlo simulations have also confirmed the energy deposition in the dielectric and electron-hole generation are significantly enhanced in high- $k$  dielectrics [51,52].

Besides the sensitivity, a long term stability of  $\Delta V_{th}$  after irradiation is also important parameter for pMOS dosimeters. The fading characteristics have been assessed during room temperature post-irradiation annealing with zero gate bias and results are shown in Fig. 6. The

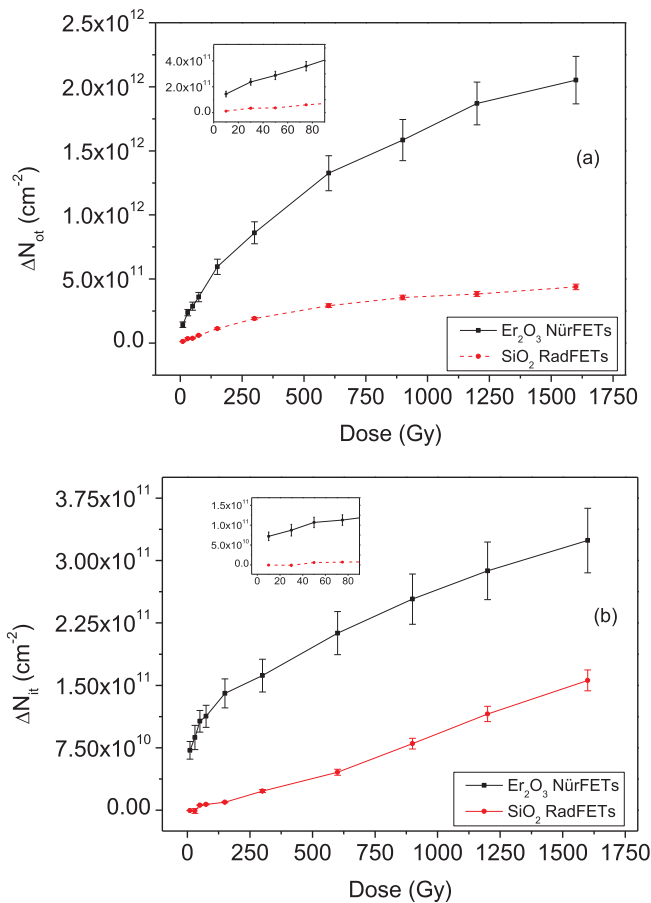


Fig. 5. Radiation induced (a) oxide trap density, and (b) interface trap density at various doses.

11.9% percentage fading after two weeks for the SiO<sub>2</sub> RadFETs is in agreement with the literature [10,53]. The Er<sub>2</sub>O<sub>3</sub> sample fading is significantly larger, exceeding 20%, which indicates the need for further optimization of this technology. The fading is mainly associated with the recombination of the trapped charge located in the shallow trap sites; this reduces the threshold voltage shift during annealing [4]. The SiO<sub>2</sub> and Er<sub>2</sub>O<sub>3</sub> dielectrics exhibited the fading characteristics, but Er<sub>2</sub>O<sub>3</sub> has somewhat larger fading values. Large numbers of the charges are trapped in both the gate dielectric and at the interface in the Er<sub>2</sub>O<sub>3</sub>

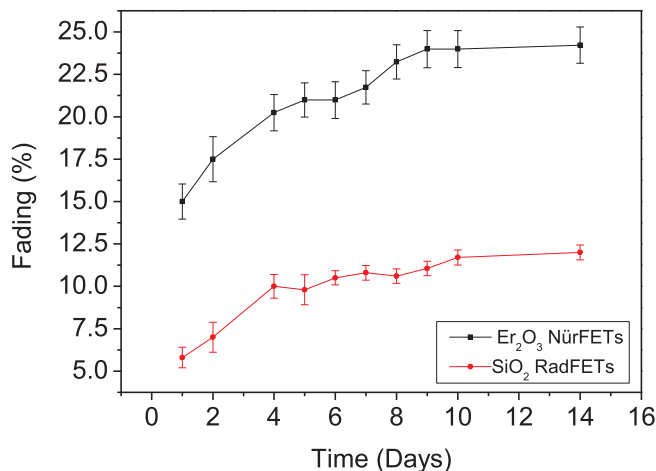


Fig. 6. The post-irradiation fading values of the Tyndall RadFETs and Er<sub>2</sub>O<sub>3</sub> NürFETs.

NürFETs. Thus, it may be usual to observe higher recombination of the trapped charges. In addition, the higher fading values of device also demonstrate that the numbers of the shallow trap states of Er<sub>2</sub>O<sub>3</sub> dielectrics are relatively higher than in the SiO<sub>2</sub> dielectric.

#### 4. Conclusion

The sensitivity of the Er<sub>2</sub>O<sub>3</sub> NürFETs has been calculated to be 15 mV/Gy vs. only 4.6 mV/Gy for SiO<sub>2</sub> RadFETs at 30 Gy. However, device sensitivities drop to 2.10 mV/Gy for Er<sub>2</sub>O<sub>3</sub> NürFETs, and 1.88 mV/Gy for SiO<sub>2</sub> RadFETs at 1600 Gy. The increased sensitivity in Er<sub>2</sub>O<sub>3</sub> samples is associated with higher Z<sub>eff</sub> number, higher density, and domination of single type of hole trapping mechanism. After 14 days room temperature annealing, 11.9% and 24.4% fading was observed in SiO<sub>2</sub> RadFETs and Er<sub>2</sub>O<sub>3</sub> NürFETs, respectively. This higher fading value for the Er<sub>2</sub>O<sub>3</sub> is associated with a higher density of generated shallow traps in the Er<sub>2</sub>O<sub>3</sub> dielectric. These obtained results have demonstrated that the performance of Er<sub>2</sub>O<sub>3</sub> as the gate dielectric in the pMOS dosimeter is advantageous, or at least comparable to that of typically used SiO<sub>2</sub>. Higher sensitivity of Er<sub>2</sub>O<sub>3</sub> devices is crucial for improved performance of the pMOS dosimeters, particularly at lower doses. In other words, it seems that minimum detectable dose can be improved by using the Er<sub>2</sub>O<sub>3</sub> dielectric layer, which can be a milestone for the pMOS dosimeters use in personal dosimetry.

#### Acknowledgments

This work was supported in part by the Ministry of Development, Turkey, under Contract 2016K121110, in part by The Scientific and Technological Research Council of Turkey (TÜBİTAK) under Contact 114F066, and in part by Abant İzzet Baysal University, Bolu, Turkey, under Contract BAP. 2015.03.02.954 and 2017.03.02.1245. This investigation forms a part of the PhD thesis of S. Kaya.

#### References

- [1] A. Holmes-Siedle, The space-charge dosimeter: General principles of a new method of radiation detection, Nucl. Instrum. Methods 121 (1974) 169–179.
- [2] Y. Kimoto, A. Jaksic, RADFET utilization for spacecraft dosimetry, Int. Conf. Microelectr. (2004) 657–659.
- [3] A. Javanainen, J.R. Schwank, M.R. Shaneyfelt, R. Harboe-Sorensen, A. Virtanen, H. Kettunen, S.M. Dalton, P.E. Dodd, A.B. Jaksic, Heavy-ion induced charge yield in MOSFETs, IEEE Trans. Nucl. Sci. 56 (2009) 3367–3371.
- [4] E. Yilmaz, A. Kahraman, A.M. McGarrigle, N. Vasovic, D. Yegen, A. Jaksic, Investigation of RadFET response to X-ray and electron beams, Appl. Radiat. Isotopes 127 (2017) 156–160.
- [5] M.S. Martinez-Garcia, J.T. del Rio, A.J. Palma, A.M. Lallena, A. Jaksic, M.A. Carvajal, Comparative study of MOSFET response to photon and electron beams in reference conditions, Sens. Actuators, A-Phys. 225 (2015) 95–102.
- [6] A. Jaksic, K. Rodgers, C. Gallagher, P.J. Hughes, Use of RADFETs for quality assurance of radiation cancer treatments, Int. Conf. Microelectr. (2006) 577–579.
- [7] M.S. Martinez-Garcia, J.T. del Rio, A. Jaksic, J. Banqueri, M.A. Carvajal, Response to ionizing radiation of different biased and stacked pMOS structures, Sens. Actuators, A-Phys. 252 (2016) 67–75.
- [8] A. Jaksic, G. Ristic, M. Pejovic, A. Mohammadzadeh, W. Lane, Characterisation of radiation response of 400nm implanted gate oxide RADFETs, Int. Conf. Microelectr. (2002) 727–730.
- [9] G.S. Ristic, N.D. Vasovic, M. Kovacevic, A.B. Jaksic, The sensitivity of 100 nm RADFETs with zero gate bias up to dose of 230 Gy(Si), Nucl. Instrum. Methods B. 269 (2011) 2703–2708.
- [10] G. Ristic, S. Golubovic, M. Pejovic, P-channel metal-oxide-semiconductor dosimeter fading dependencies on gate bias and oxide thickness, Appl. Phys. Lett. 66 (1995) 88–89.
- [11] G. Ristic, A. Jaksic, M. Pejovic, pMOS dosimetric transistors with two-layer gate oxide, Sens. Actuators, A-Phys. 63 (1997) 129–134.
- [12] A. Jaksic, Y. Kimoto, V. Ogourtsov, V. Polischuk, A. Mohammadzadeh, A. Mathewson, The effect of different biasing configurations on RADFET response measured by automated read-out system, ESA Sp. Publ. 536 (2004) 489–492.
- [13] A. Haran, A. Jaksic, The role of fixed and switching traps in long-term fading of implanted and unimplanted gate oxide RADFETs, IEEE Trans. Nucl. Sci. 52 (2005) 2570–2577.
- [14] G. Ristic, S. Golubovic, M. Pejovic, Sensitivity and fading of pMOS dosimeters with thick gate oxide, Sens. Actuators, A-Phys. 51 (1995) 153–158.
- [15] E. Yilmaz, I. Dogan, R. Turan, Use of Al<sub>2</sub>O<sub>3</sub> layer as a dielectric in MOS based radiation sensors fabricated on a Si substrate, Nucl. Instrum. Methods B 266 (2008)

- 4896–4898.
- [16] S. Kaya, E. Yilmaz, A. Kahraman, H. Karacali, Frequency dependent gamma-ray irradiation response of  $\text{Sm}_2\text{O}_3$  MOS capacitors, *Nucl. Instrum. Methods B* 358 (2015) 188–193.
- [17] A. Kahraman, E. Yilmaz, A. Aktag, S. Kaya, Evaluation of radiation sensor aspects of  $\text{Er}_2\text{O}_3$  MOS capacitors under zero gate bias, *IEEE Trans. Nucl. Sci.* 63 (2016) 1284–1293.
- [18] D.R. Dance, S. Christofides, A.D.A. Maidment, I.D. McLean, K.H. Ng, *Diagnostic Radiology Physics: A Handbook for Teachers and Students*, Int. At. Energy Agency (2014).
- [19] G. Lupina, T. Schroeder, C. Wenger, J. Dabrowski, H.J. Mussig, Thermal stability of Pr silicate high-k layers on Si(001), *Appl Phys Lett.* 89 (2006).
- [20] S.J. Jo, J.S. Ha, N.K. Park, D.K. Kang, B.H. Kim, 5 nm thick lanthanum oxide thin films grown on Si(100) by atomic layer deposition: The effect of post-annealing on the electrical properties, *Thin Solid Films* 513 (2006) 253–257.
- [21] M. Leskela, K. Kukli, M. Ritala, Rare-earth oxide thin films for gate dielectrics in microelectronics, *J. Alloy Compd.* 418 (2006) 27–34.
- [22] T.M. Pan, W.S. Huang, Physical and electrical characteristics of a high-k  $\text{Yb}_2\text{O}_3$  gate dielectric, *Appl Surf Sci.* 255 (2009) 4979–4982.
- [23] Y.Y. Zhu, S. Chen, R. Xu, Z.B. Fang, J.F. Zhao, Y.L. Fan, X.J. Yang, Z.M. Jiang, Band offsets of  $\text{Er}_2\text{O}_3$  films epitaxially grown on Si substrates, *Appl. Phys. Lett.* 88 (2006).
- [24] A. Tursucu, D. Demir, P. Onder, Effective atomic number determination of rare earth oxides with scattering intensity ratio, *Sci. Technol. Nucl. Installations* (2013).
- [25] A. Ortiz-Conde, F.J.G. Sanchez, J.J. Liou, A. Cerdeira, M. Estrada, Y. Yue, A review of recent MOSFET threshold voltage extraction methods, *Microelectron. Reliab.* 42 (2002) 583–596.
- [26] P.J. Mcwhorter, P.S. Winokur, Simple technique for separating the effects of interface traps and trapped-oxide charge in metal-oxide-semiconductor transistors, *Appl. Phys. Lett.* 48 (1986) 133–135.
- [27] G. Lucovsky, G.B. Rayner, D. Kang, C.L. Hinkle, J.G. Hong, A spectroscopic phase separation study distinguishing between chemical with different degrees of crystallinity in Zr(Hf) silicate alloys, *Surf. Sci.* 566 (2004) 772–776.
- [28] G. Lucovsky, D.M. Fleetwood, S. Lee, H. Seo, R.D. Schrimpf, J.A. Felix, J. Luning, L.B. Fleming, M. Ulrich, D.E. Aspnes, Differences between charge trapping states in irradiated nano-crystalline  $\text{HfO}_2$  and non-crystalline Hf silicates, *IEEE Trans. Nucl. Sci.* 53 (2006) 3644–3648.
- [29] A. Kahraman, E. Yilmaz, S. Kaya, A. Aktag, Effects of post deposition annealing, interface states and series resistance on electrical characteristics of  $\text{HfO}_2$  MOS capacitors, *J. Mater. Sci.-Mater. Electron.* 26 (2015) 8277–8284.
- [30] D. Aryanto, W.N. Jannah, T. Masturi, A.S. Sudiro, P. Sebayang Wismogroho, P. Marwoto Sugianto, Preparation and structural characterization of ZnO thin films by sol-gel method, *J. Phys. Conf. Ser.* 817 (2017).
- [31] F. Karaboga, H. Yetis, M. Oz, I. Belenli, Effect of different-sized h-BN nano-particles on some properties of  $\text{MgB}_2$  superconductors, *J. Mater. Sci.-Mater. Electron.* 27 (2016) 8512–8517.
- [32] C.H. Kao, H. Chen, Y.T. Pan, J.S. Chiu, T.C. Lu, The characteristics of the high-K  $\text{Er}_2\text{O}_3$  (erbium oxide) dielectrics deposited on polycrystalline silicon, *Solid State Commun.* 152 (2012) 504–508.
- [33] V. Mikhelashvili, G. Eisenstein, F. Edelman, R. Brenner, N. Zakharov, P. Werner, Structural and electrical properties of electron beam gun evaporated  $\text{Er}_2\text{O}_3$  insulator thin films, *J. Appl. Phys.* 95 (2004) 613–620.
- [34] A.K. Rana, N. Chand, V. Kapoor, Impact of gate engineering on gate leakage behavior of nano scale MOSFETs with High-k dielectrics, *J. Nanoelectron. Optoelectron.* 5 (2010) 343–348.
- [35] M. Gurfinkel, J.S. Suehle, Y. Shapira, Enhanced gate induced drain leakage current in  $\text{HfO}_2$  MOSFETs, *Microelectron. Eng.* 86 (2009) 2157–2160.
- [36] A.O. Cetinkaya, S. Kaya, A. Aktag, E. Budak, E. Yilmaz, Structural and electrical characterizations of  $\text{BiFeO}_3$  capacitors deposited by sol-gel dip coating technique, *Thin Solid Films* 590 (2015) 7–12.
- [37] R.W. Johnson, A. Hultqvist, S.F. Bent, A brief review of atomic layer deposition: from fundamentals to applications, *Mater. Today* 17 (2014) 236–246.
- [38] A. Cabrero-Vilatela, J.A. Alexander-Webber, A.A. Sagade, A.I. Aria, P. Braeuninger-Weimer, M.B. Martin, R.S. Weatherup, S. Hofmann, Atomic layer deposited oxide films as protective interface layers for integrated graphene transfer, *Nanotechnology* 28 (2017).
- [39] M.M. Giangregorio, A. Sacchetti, M. Losurdo, P. Capezzuto, G. Bruno, Correlation between structure and properties of  $\text{Er}_2\text{O}_3$  nanocrystalline thin films, *J. Non-Cryst. Solids* 354 (2008) 2853–2857.
- [40] S. Kaya, E. Yilmaz, Influences of Co-60 gamma-ray irradiation on electrical characteristics of  $\text{Al}_2\text{O}_3$  MOS capacitors, *J. Radioanal. Nucl. Chem.* 302 (2014) 425–431.
- [41] G.S. Ristic, Influence of ionizing radiation and hot carrier injection on metal-oxide-semiconductor transistors, *J. Phys. D Appl. Phys.* 41 (2008).
- [42] T.P. Ma, P.V. Dressendorfer, *Ionizing Radiation Effects in MOS Devices and Circuits*, Wiley & Sons, 1989.
- [43] S. Kaya, E. Yilmaz, Modifications of structural, chemical, and electrical characteristics of  $\text{Er}_2\text{O}_3/\text{Si}$  interface under Co-60 gamma irradiation, *Nucl. Instrum. Methods B* 418 (2018) 74–79.
- [44] A.S. Foster, F.L. Gejo, A.L. Shluger, R.M. Nieminen, Vacancy and interstitial defects in hafnia, *Phys. Rev. B.* 65 (2002).
- [45] T.R. Oldham, F.B. McLean, Total ionizing dose effects in MOS oxides and devices, *IEEE Trans. Nucl. Sci.* 50 (2003) 483–499.
- [46] S. Kaya, A. Jaksic, E. Yilmaz, Co-60 gamma irradiation effects on electrical characteristics of  $\text{HfO}_2$  MOSFETs and specification of basic radiation-induced degradation mechanism, *Radiat. Phys. Chem.* 149 (2018) 7–13.
- [47] S.K. Dixit, X.J. Zhou, R.D. Schrimpf, D.M. Fleetwood, S.T. Pantelide, R. Choi, G. Bersuker, L.C. Feldman, Radiation induced charge trapping in ultrathin  $\text{HfO}_2$ -based MOSFETs, *IEEE Trans. Nucl. Sci.* 54 (2007) 1883–1890.
- [48] C.Z. Zhao, S. Taylor, M. Werner, P.R. Chalker, R.J. Potter, J.M. Gaskell, A.C. Jones, High-k materials and their response to gamma ray radiation, *J. Vac. Sci. Technol. B.* 27 (2009) 411–415.
- [49] N. Manikantababu, N. Arun, M. Dhanunjaya, V. Saikiran, S.V.S.N. Rao, A.P. Pathak, Synthesis, characterization and radiation damage studies of high-k dielectric ( $\text{HfO}_2$ ) films for MOS device applications, *Radiat. Eff. Defect Solids* 170 (2015) 207–217.
- [50] A. Kahraman, E. Yilmaz, Irradiation response of radio-frequency sputtered Al/ $\text{Gd}_2\text{O}_3$ /p-Si MOS capacitors, *Radiat. Phys. Chem.* 139 (2017) 114–119.
- [51] A. Dasgupta, D.M. Fleetwood, R.A. Reed, R.A. Weller, M.H. Mendenhall, B.D. Sierawski, Dose enhancement and reduction in  $\text{SiO}_2$  and high-kappa MOS insulators, *IEEE Trans. Nucl. Sci.* 57 (2010) 3463–3469.
- [52] A. Kahraman, S. Kaya, A. Jaksic, E. Yilmaz, A comprehensive study on the photon energy response of RadFET dosimeters using the PENELOPE Monte Carlo code, *Radiat. Eff. Defect Solids* 170 (2015) 367–376.
- [53] M.M. Pejovic, M.M. Pejovic, A.B. Jaksic, Response of pMOS dosimeters on gamma-ray irradiation during its re-use, *Radiat. Prot. Dosim.* 155 (2013) 394–403.